Lattices (Clarendon, Oxford, England, 1954), p. 134ff.

[16]Had an optic mode of the type governed by Eq. (1) provided the primary instability, secondary distortions involving *both* tetragonal strains and $\Gamma_{12}(+)$ sublattice displacements would have resulted. However, inspection shows that arbitrary $\Gamma_{12}(+)$ displacements may be added to those listed in Table I without further lowering the symmetry of the space group.

[17]P. B. Miller and J. D. Axe, Phys. Rev. 163, 924 (1967).

PHYSICAL REVIEW B VOLUME 4, NUMBER 9 1 NOVEMBER 1971

Finite-Voltage Behavior of Lead-Copper-Lead Junctions*

John Clarke†

Department of Physics, University of California, Berkeley, California 94720
and Inorganic Materials Research Division, Lawrence Radiation Laboratory, Berkeley, California 94720

(Received 9 June 1971)

Pb-Cu-Pb junctions were made by evaporating successively on to a glass substrate a strip of Pb, a disk of Cu, and a second strip of Pb at right angles to the first. Each Pb strip had a width w. At liquid-He^4 temperatures, the junctions could sustain a dc Josephson supercurrent less than or equal to the critical current i_c. When i_c was small enough so that the Josephson penetration depth λ_J ($\propto i_c^{-1/2}$) was greater than $\frac{1}{4}w$, the supercurrent flowed uniformly through the junction, which was said to be "weak." When i_c was higher so that λ_J was less than $\frac{1}{4}w$, the supercurrents were nonuniform, and the junction was said to be "strong." At a current i greater than i_c, the voltage v across a weak junction was in reasonable agreement with the theoretical result $v=(i^2-i_c^2)^{1/2}R$, where R is the normal-state resistance of the Cu film. For strong junctions, a dc supercurrent appeared at finite voltages, because the ac supercurrents had a nonzero time average. The experimental results are in good qualitative agreement with calculations on a one-dimensional model. When the current was fed into the junction asymmetrically, that is, when it was applied to one end of each Pb strip, the self-field of the current generated periodic structure on the i-v characteristic, the period being typically 3 mA. The structure vanished if the currents were applied symmetrically, that is, the input and output currents divided equally between the ends of each lead strip. The application to a junction of rf electromagnetic radiation of angular frequency Ω induced constant-voltage current steps at voltages $(n/m)\hbar\Omega/(2e)$, where n and m are integers. The amplitude of the steps was modulated by the amplitude of the rf power and by a magnetic field in approximately the manner observed in tunnel junctions with oxide barriers. The dynamic resistance of the steps was less than $1.7\times10^{-14}\,\Omega$. The electrochemical potential across the junction at which a given step appeared was not affected by either junction material or experimental conditions at a precision of 1 part in 10^8. The highest frequency at which steps were induced was 2 MHz. At this frequency the skin depth of the copper was much less than w, and little radiation was coupled into the junction. The lowest frequency was 5 kHz, corresponding to a first-order induced step at about 10^{-11} V. At this voltage, the Johnson-noise broadening of the Josephson frequency was also about 5 kHz. At lower frequencies, the noise completely destroyed the synchronization between the Josephson ac supercurrents and the rf radiation, so that no steps were observed.

I. INTRODUCTION

An *SNS* junction consists of a thin film of a normal metal sandwiched between two superconductors. Each superconductor induces into the normal metal a finite pair amplitude[1-3] which decays exponentially[1-3] towards the middle of the normal layer. Provided the normal metal is not too thick, the overlap of the two pair wave functions will be large enough for the coupling energy[4,5] of the two superconductors to exceed the thermal fluctuation energy.[5-7] As a result, phase coherence will be established across the junction, and Josephson[5,7,8] tunneling becomes possible. It should be pointed out that the passage of a supercurrent through an *SNS* junction does in fact require a pair *tunneling* process. Although there are one-electron propagating states in the normal metal, the pairs induced in each side of the normal layer by the superconductors are in evanescent states,[2] and cannot support a supercurrent unless the two decaying wave functions overlap. Under these circumstances, the supercurrent i obeys the Josephson[6,9] current phase relation

$$i=i_c\sin\phi\,, \tag{1.1}$$

where i_c is the critical current (maximum supercurrent) and ϕ is the phase difference between the

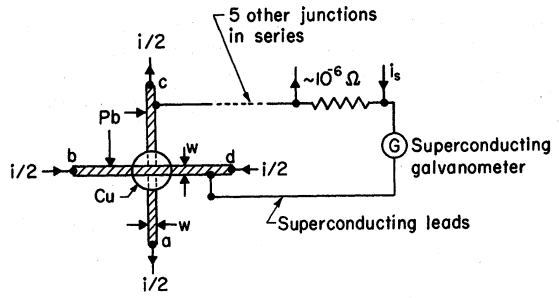

FIG. 1. Configuration of Pb-Cu-Pb junction and measuring circuit.

order parameters of the two superconductors.

The supercurrent-carrying properties of Pb-Cu-Pb junctions have been described in detail in an earlier paper,[10] which will be referred to as I. In that investigation, 3% of aluminum was dissolved in the Cu, so that the normal layer was in the dirty limit. The main results discussed in I were as follows.

(i) The critical current $i_c(T)$, assuming a uniform current distribution over the junction, could be adequately represented by an equation of the form[2,10]

$$i_c(T) = f(T)e^{-2k_N a}. \tag{1.2}$$

The thickness of the normal layer is $2a$. The decay length in the normal metal for the dirty limit ($l \ll k_N^{-1}$) is given by[2]

$$k_N^{-1} = (\hbar v_{FN} l_N / 6\pi kT)^{1/2} \quad (l \ll k_N^{-1}), \tag{1.3}$$

where v_{FN} is the Fermi velocity, l_N is the electronic mean free path, and T is the temperature of the junction. Equation (1.3) assumes that the transition temperature of the Cu:Al, T_{cN}, is close to zero. Near the transition temperature of the superconductors, T_{cS}, $f(T)$ is proportional[2] to $(1 - T/T_{cS})^2$. For temperatures below about $\frac{1}{2}T_{cS}$, $f(T)$ is nearly independent of temperature.

(ii) The junctions were fabricated in the crossed film geometry of Fig. 1. The current i was fed into the junction either in an asymmetric configuration, by using terminals a and b of Fig. 1, or in a symmetric configuration, by dividing the input current equally between b and d, and the output between a and c. It was found that the measured critical current was the same for the two cases provided that the Josephson penetration depth λ_J was $\gtrsim \frac{1}{4}w$, where w is the junction width. For $\lambda_J \lesssim \frac{1}{4}w$, self-field limiting[5,6,11] occurs, even for the symmetric configuration. (Notice that in a self-field limited junction, the current flows in an effective skin depth $2\lambda_J$.) The Josephson penetration depth is defined as[5,6,11]

$$\lambda_J = [\hbar c^2 / 16\pi(a+\lambda)eI_c]^{1/2}, \tag{1.4}$$

where λ is the penetration depth of the superconductor[12] and I_c is the critical current density. A junction for which $\lambda_J \gtrsim \frac{1}{4}w$ is said to be *weak* or *small*, whereas one for which $\lambda_J \lesssim \frac{1}{4}w$ is said to be *strong* or *large*.

(iii) The critical current was modulated by a magnetic field applied in the plane of the normal film. For weak junctions, the critical-current dependence on the magnetic field exhibited the well-known Fraunhofer pattern.[4] In the case of strong junctions, the dependence of critical current upon the field was modified, exhibiting a linear region near $H = 0$. This behavior was in excellent agreement with the calculation of Owen and Scalapino.[13]

Bondarenko, Dmitrenko, and Balanov[14] have studied *SNS* junctions in which the normal metal is in the clean limit ($l \gg k_N^{-1}$). They found that $k_N^{-1} = \hbar v_{FN}/2\pi kT$, in accordance with the prediction of de Gennes.[3]

This paper is concerned with the properties of *SNS* junctions when they are in a finite-voltage regime, i.e., when the current through them exceeds the critical current. Much of the theory of this dissipative state has been discussed in detail in an article by Waldram, Pippard, and Clarke.[15] This paper will be referred to as II. We shall quote a number of results from II without repeating their derivations. We shall be concerned with three main features: the shape of the current-voltage (i-v) characteristics, which is described in Sec. III and compared with theoretical predictions for both weak and strong junctions; the self-modulation of the i-v characteristic, described in Sec. IV; finally, the properties of constant-voltage current steps induced on the i-v characteristic by rf radiation, discussed in Sec. V.

II. JUNCTION PREPARATION AND MEASUREMENT

Specimen preparation was very similar to that described in I. A 7000-Å strip of Pb (0.2 mm wide), a disk of Cu or Cu:Al (5 mm in diameter), and a second strip of Pb at right angles to the first were evaporated successively onto a glass slide (see Fig. 1). The junction area (w^2) was thus about 4×10^{-4} cm^2. The thicknesses of Cu:Al were in the range 5000–7000 Å, whereas those of pure Cu were in the range 10 000–14 000 Å. A greater thickness of pure Cu was possible because, at a given temperature, the pair-decay length in pure Cu was greater than that in the alloy. In the clean limit, $k_N^{-1} \sim 1\ \mu$ at 1 K. The mean free path of the pure Cu at low temperatures was typically 5000 Å, so that the material was relatively clean at 4 K and relatively dirty at 1 K. Specimens with pure Cu barriers were less reproducible than those with Cu:Al barriers, probably because the effects of diffusion

were more significant in the clean case.

Six specimens were evaporated on each glass slide and connected in series (Fig. 1). The normal-state differential resistance was from 10^{-6} to 10^{-7} Ω. The i-v characteristic of each junction was determined by passing a current from a high impedance source through it and measuring the voltage developed by means of a superconducting galvanometer[16] in series with a standard resistance of about 10^{-6} Ω. The voltage across each junction was balanced by a current i_s in the standard resistance. This null-reading technique minimized the loading of the junction by the voltmeter so that junction was supplied effectively by a current source. The voltage resolution was 10^{-13} V and the measurement time constant 0.2 sec (limited by room-temperature instrumentation).

The specimens were immersed in liquid helium, the temperature of which was stabilized in the range 1.2–4.2 K by a device designed by Rochlin.[17] The junctions and voltmeter were enclosed in a superconducting can, and the cryostat surrounded by a double μ-metal can which reduced the ambient magnetic field to less than 5 mG. Two coaxial solenoids were mounted inside the superconducting can around the specimens. One was used to apply uniform magnetic fields of up to a few gauss in the plane of the junction and the other to apply rf fields in order to induce steps on the i-v characteristic.

III. CURRENT-VOLTAGE CHARACTERISTICS

A. Normal Current Flow

First, let us briefly discuss the passage of a normal current through an *SNS* junction with a finite voltage across it.

If the normal metal is sufficiently thick, and the temperature sufficiently high, the coupling energy of the junction[4,5] $i_c\phi_0/2\pi$ becomes comparable with kT.[18] Under these circumstances, fluctuations decouple the phase coherence of the two superconductors and the junction becomes "normal." We need to know the resistance of the junction in this normal state. Experimentally, if the mean free path of the normal layer is deliberately shortened by alloying, the measured resistance is approximately equal to the Ohmic resistance of the normal slab,[10] provided $T \lesssim \frac{1}{2}T_{cS}$. This result suggests that the conversion from quasiparticle current in the normal metal to superfluid current in the superconductor occurs at or very close to the *SN* interface. The following model[19] accounts for this result.

Assume that the BCS[20] interaction parameter V in copper is zero. There will still be an appreciable pair-condensation amplitude F_N induced in the Cu by the Pb, but the pair potential, $\Delta_N = V_N F_N$, will be zero everywhere in the Cu.[2] Consider an electron propagating in the Cu towards the *SN* interface, with an energy less than the pair potential in the superconductor at the interface, $\Delta_S^{(i)}$. The electron will suffer Andreev scattering[21] at the interface, and a hole will be reflected back into the Cu while a condensed pair propagates into the Pb. The conversion from normal to superflow consequently occurs at the interface. If V_N is in fact finite but very small in the range 1–4 K, Δ_N will everywhere be small compared with typical electron energies kT and the resistance will not be appreciably different. If the temperature of the junction is raised appreciably above $\frac{1}{2}T_{cS}$, $\Delta_S^{(i)}$ begins to fall while the electron thermal energies increase. Electrons with energies above $\Delta_S^{(i)}$ will now have a finite probability[22] of propagating into the superconductor where they will decay dissipatively.[23] The measured resistance will rise accordingly.[24] Finally, it should be noted that if the barrier is of pure Cu, lead diffusing in near the boundary regions will have an appreciable effect on the mean free path. The measured resistance will be higher than the expected resistance of the Cu slab.

It appears that the normal current flow through the barrier is quite unaffected by the presence of a condensation amplitude. We shall assume that this result remains true even if the barrier is made thinner so that Josephson tunneling occurs. We assume that once the total current exceeds the critical current, and a voltage is developed across the junction, the barrier current has two components, one a normal current obeying Ohm's law, and the other an oscillating supercurrent obeying Josephson's equations. We shall see presently that the asymptotic *dynamic* resistance of the junction is quite independent of the coupling energy of the junction, so that our assumption is justified.

B. Small Junction Limit

In the limit $\lambda_J \gtrsim \frac{1}{4}w$ the current flows uniformly through the junction. We assume that if the current is supplied from a high-impedance source, the total current i may be expressed in the form[15]

$$i = i_c \sin\phi + \frac{v}{R} = i_c \sin\phi + \frac{\hbar}{2eR}\frac{d\phi}{dt}\ , \qquad (3.1)$$

where we have used[8] $v = (\hbar/2e)d\phi/dt$. The resistance of the junction is R and its critical current i_c. We have neglected the junction capacitance, which is of order 1 pF. The highest Josephson frequencies likely to occur in an *SNS* junction are of order 50 MHz (corresponding to voltages of 10^{-7} V) so that the lowest parallel reactance of the capacitance is greater than 1 KΩ. This value is quite negligible compared with the barrier resistance of 1 μΩ or less.

We are required to solve Eq. (3.1) for the time-averaged voltage as a function of i. The solution

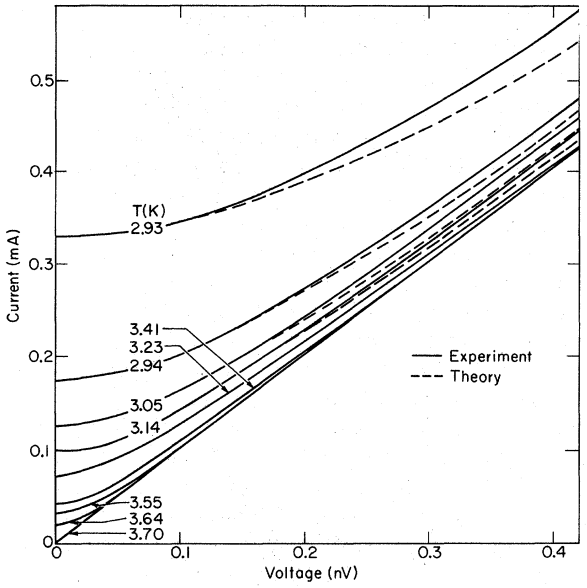

FIG. 2. Experimental and theoretical plots for the i-v characteristics of a weak *SNS* junction. For the highest critical current, $w/\lambda_J \simeq 1.3$.

has been given by several authors[15,25,26] and is

$$\bar{v} = (i^2 - i_c^2)^{1/2} R \ . \tag{3.2}$$

Experimental i-v characteristics for a small junction at several temperatures are shown as solid curves in Fig. 2. The current was supplied from a high-impedance source. For reasons explained in detail in Sec. IV, a symmetric current feed was used. The theoretical curves in Fig. 2 were calculated by using the measured resistance at 3.70 K and the measured value of i_c. The agreement between theory and experiment is good for the lower values of critical current. However, for the highest value of critical current, for which $w/\lambda_J \simeq 1.3$, the measured current is somewhat higher than the calculated value for voltages above 0.1 nV. There are at least two possible reasons for this distortion of the characteristic. First, it is possible that a small amount of flux flow has set in at this rather low value of w/λ_J (see Sec. III C). The flux flow would tend to increase the total current at finite voltages, as is observed. The second possibility is that self-modulation effects are distorting the characteristic (see Sec. IV).

It should be emphasized that these i-v characteristics obtained with a current source are qualitatively quite different from what one would obtain with a voltage source. With a voltage source, the phase difference ϕ always increases uniformly with time at finite voltages and the time-averaged supercurrent $\langle i_c \sin\phi \rangle$ is zero. The characteristic would (ideally) consist of a zero-voltage spike and a straight line representing the resistance through the origin. With a current source, ϕ does not increase uniformly with time, as can be seen by rewriting Eq. (3.1) in the form $d\phi/dt = 2eR \times (i - i_c \sin\phi)/\hbar$. The junction spends more time in the forward-supercurrent condition $[2n\pi \leq \phi \leq (2n+1)\pi]$ than in the backward-supercurrent condition $[(2n+1)\pi \leq \phi \leq (2n+2)\pi]$. The supercurrent at finite voltages is no longer a sinusoidal function of time and its time average becomes nonzero. Consequently, there is a finite dc supercurrent for small values of voltage but, as the current is increased, the dc supercurrent tends asymptotically to zero.

C. Large Junction Limit

When $\lambda_J \ll w$, we can no longer assume that the electromagnetic fields and phase difference ϕ are the same at all points in the barrier. In order to make the calculations tractable, we take as our model a one-dimensional junction, the barrier of which lies in the x-y plane (see Fig. 3). The junction is very long in the y direction. A magnetic field H parallel to the y axis gives rise to a spatial dependence[5,6] of ϕ, $\partial\phi/\partial x = 4e(a+\lambda)H/(\hbar c)$. Combining this relation with Eq. (3.1) and Ampère's law, $\partial H/\partial x = 4\pi i/c$, we obtain (using current densities)

$$\lambda_J^2 \frac{\partial^2\phi}{\partial x^2} = \sin\phi + \frac{\hbar}{2eRI_c}\frac{\partial\phi}{\partial t} \ . \tag{3.3}$$

For currents below the critical current, Eq. (3.3) reduces to the well-known equation $\lambda_J^2 \partial^2\phi/\partial x^2 = \sin\phi$, which has been thoroughly studied.[10,13,27-29] In the absence of applied currents and for small applied fields, the junction will exhibit the Meissner effect and screening currents will flow on each side of the junction in a penetration depth $2\lambda_J$. For fields greater than[10] $\pi H_{c_1}/2 = 8\pi\lambda_J I_c/c$, vortices will enter the junction, each vortex containing one quantum of flux, ϕ_0. A vortex is simply a region over which the phase difference ϕ across the junction changes by 2π. The self-field of the applied current may also generate vortices, whether or not there is an additional applied magnetic field.

When there is a finite voltage across the junction, these vortices will move. Unfortunately, Eq. (3.3) has no analytic solutions for finite values of $\partial\phi/\partial t$ and we have been forced to solve it numerically for the time-averaged voltage.[15] Solutions are shown in Fig. 4(a) for various values of w/λ_J. For $w/\lambda_J \gtrsim 4$, there is a finite dc supercurrent which persists to high voltages. This supercurrent arises from the vortex motion in the following way. If the flux motion is driven by a current applied symmetrically (as in Fig. 3), flux lines of opposite sign will enter the junction at the edges and flow into the center, where they

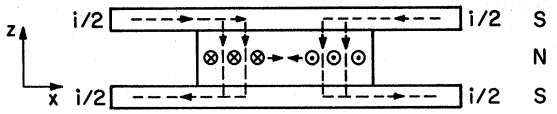

FIG. 3. Section in the (x, z) plane of a one-dimensional junction which is very long in the y direction. Currents fed symmetrically into the junction create flux lines of opposing sign near the edge of the junction. At finite voltages, the lines move into the center, where they mutually annihilate.

will annihilate one another. In order for the flux lines to move, there must be a gradient of flux line density across the junction. The density of vortices will be highest near the edges of the junction and lowest near the center, where they are moving rapidly towards annihilation. (These results are illustrated by photographs of a mechanical analog in II.) If we consider a point near one edge of a barrier containing many vortices, the closely packed moving flux lines constitute an almost uniform magnetic field. The voltage produced is just $\nu\phi_0$, where ν is the number of flux lines crossing the point per second, and ϕ_0 is the flux quantum. This voltage is constant in time, ϕ increases linearly with time, and there is no dc supercurrent. The junction in this region is normal in the sense that the electric field arises in the same way as it does in any conductor carrying a current.

On the other hand, at a point near the center of the junction, the flux lines are widely spaced and moving rapidly. Consequently, ϕ increases with time in a very nonuniform manner and the time-averaged supercurrent is finite. Thus the dc supercurrent at finite voltages tends to flow in the interior of the junction. Our calculations in II indicate that about one-half of the zero-voltage supercurrent should persist to high voltages.

The comparison of this long-junction model with experimental junctions is confused because data are available only for square junctions. Results obtained for values of w/λ_J between 2.0 and 7.2 are shown in Fig. 4(b), and for values between 2.0 and 17.6 in Fig. 4(c). Symmetric current inputs were used. The value of w/λ_J was increased by lowering the temperature of the junction, thereby increasing the critical current.[30] The theoretical curves of Fig. 4(a) have been fitted to a one-dimensional junction of the same width and area as the square junction of Fig. 4(b). Two main differences between experiment and theory are evident. First, there is a significant finite-voltage supercurrent which persists to high voltages for $w/\lambda_J = 2.5$ [see Fig. 4(b)], whereas this behavior is not observed on the theoretical curves until w/λ_J exceeds 4. Figure 4(b) implies that, for the experimental square junctions, flux flow begins when

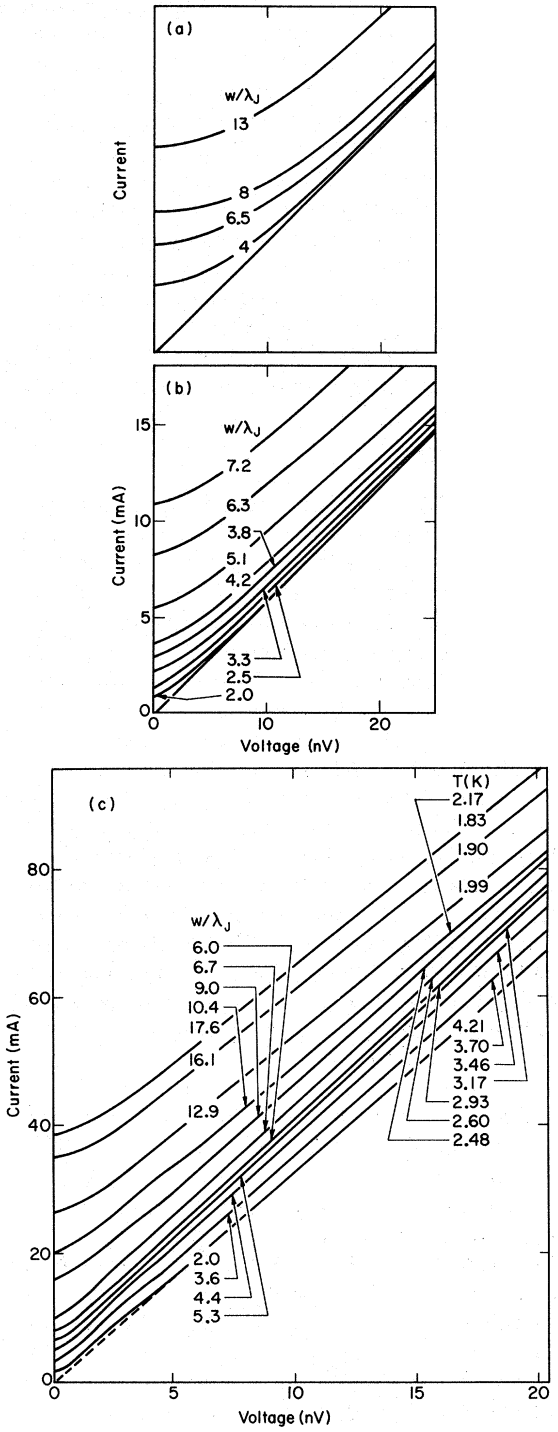

FIG. 4. (a) Theoretical i-v characteristics for the one-dimensional junction of Fig. 3, for various values of w/λ_J. The width and area have been chosen to be the same as those of the two-dimensional experimental junction in (b). Note that flux flow begins at $w/\lambda_J \sim 4$. (b) and (c) Experimental i-v characteristics for two 0.2-mm-square junctions. w/λ_J was increased by lowering the temperature. The curve of (b) corresponds to the theoretical curve of (a): Note that flux flow appears to begin at $w/\lambda_J \sim 2$.

w/λ_J is about 2. This fact may explain the distortion of the i-v characteristic referred to for small junctions in connection with Fig. 2. Second, the magnitude of the dc supercurrent at finite voltages is larger than predicted by the one-dimensional model: For the larger values of w/λ_J [Fig. 4(c)], it is almost equal to the zero-voltage supercurrent. Both effects probably arise from the two-dimensional nature of the experimental junctions in which the pattern of flux flow is not understood. The flux lines are probably more like circles which shrink and collapse on themselves in the center of the junction. The movement of these "flux circles" may initiate at the corners of the square junction, where the current density is higher than elsewhere. For this reason, the onset of flux flow may occur at relatively low values of w/λ_J.

The effect of a magnetic field applied in the plane of the junction is illustrated in Fig. 5 for a junction with $w/\lambda_J = 5.1$. The magnetic field reduces both the critical current and the finite-voltage supercurrent. However, the finite-voltage supercurrent for the lower critical currents appears to be somewhat higher than that for critical currents of the same magnitude in zero field [cf. Fig. 4(b)]. To facilitate comparison, values of *apparent* w/λ_J have been calculated for Fig. 5 from the observed critical current. The true value of w/λ_J is not changed, of course, by the magnetic field. There appears to be significant flux flow for w/λ_J as low as 1.4. This effect probably arises from the fact that the vortices are moving in two dimensions while the magnetic field is applied in one dimension. These parts of the vortex lines moving at right angles to the applied field may be less affected by it and still able to contribute a sizable supercurrent.

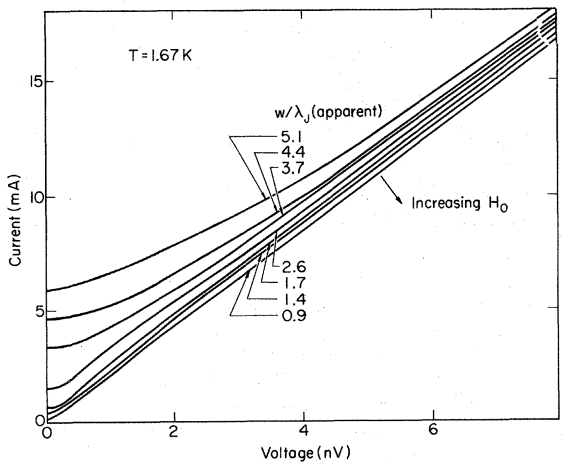

FIG. 5. Effect of magnetic field upon i-v characteristic. Values of apparent w/λ_J were calculated from the observed critical current. Notice that there is significant flux flow for w/λ_J as low as 1.4.

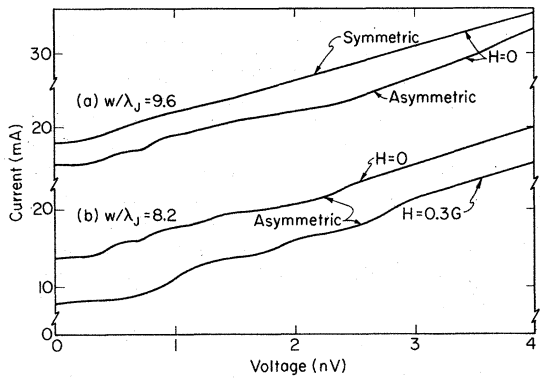

FIG. 6. Self-field modulation of i-v characteristic. (a) The effect is present for asymmetric current inputs but not for symmetric inputs. (b) Both curves are for asymmetric inputs, the effect of a magnetic field is shown.

Despite the confusion of two-dimensional junctions and a one-dimensional theory, it appears that the finite-voltage behavior of the junctions is qualitatively well understood. Quantitative predictions of the value of w/λ_J at which flux flow begins and of the magnitude of the finite-voltage supercurrent are both within a factor of 2. It would be of considerable interest to make experimental junctions which are effectively one dimensional to see if better agreement with the theory is obtained.

D. Hysteresis

No hysteresis has ever been observed in an *SNS* junction, to within the experimental error. This observation is in agreement with the calculations of McCumber[31] and Stewart,[32] who show that no hysteresis is expected in a junction for which $\beta_c = 2ei_cCR^2/\hbar$ is small compared with unity (according to Stewart, a junction with $\beta_c \sim \frac{1}{4}$ would not show hysteresis). For an *SNS* junction, if we take the junction capacitance $C \sim 1$ pF, its resistance, $R \sim 10^{-6}\ \Omega$, and $i_c \sim 1$ mA, we find $\beta_c \sim 10^{-12}$.

IV. SELF-MODULATION OF THE i-v CHARACTERISTIC

Oscillations were observed in the i-v characteristics of junctions with asymmetric current feeds, provided the critical current was greater than a few mA. Examples are shown in Fig. 6. The period is typically 2–3 mA. The oscillations disappeared when the junction was fed symmetrically (notice that the critical current for the symmetric case is higher than that for the asymmetric case[10]). The shape and position of the oscillations were changed by the application of a magnetic field in the plane of the junction (see Fig. 6). The applied field corresponds to about three flux quanta. However, the critical current has not been reduced to zero because the junction is still in the "Meissner region,"[10] i.e., the critical current still has a

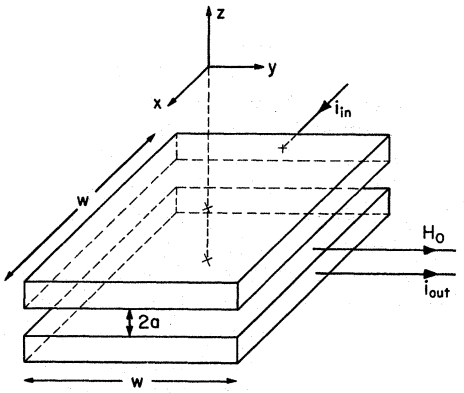

FIG. 7. Geometry of square junction, of side w. The barrier lies in the x-y plane and is of thickness $2a$. A magnetic field H_0 may be applied along the y axis.

linear dependence on field.

These oscillations arise from the self-modulation of the current flowing through the junction. A related effect for multiple junctions has been reported in an earlier paper[33] by Clarke and Fulton. The effects of self-field on the critical current of single junctions have been studied in detail by several authors.[13,27-29,34,35] If the junctions are self-field limited, the critical current may be significantly reduced by the self-field; in addition, the shape of the critical current vs magnetic field plot becomes heavily skewed. As has been shown in Sec. III C, the time-averaged current flowing in a strong junction at finite voltages contains a substantial contribution from the ac supercurrent. This supercurrent will be modulated by the self-field of the *total* current flowing through the junction. The amplitude of the oscillations cannot be properly explained, but the following model explains qualitatively all the observed features.

Consider first the effect of the self-field on the critical current of the junction. The junction configuration is indicated in Fig. 7. The junction is in the x-y plane and occupies the region $|x|, |y| \leq \frac{1}{2}w$. In the asymmetric case, current flows into the upper superconductor of the junction in the x direction and is extracted from the lower superconductor in the y direction. A magnetic field H_0 can be applied in the y direction. We assume that, in the absence of an applied magnetic field, the current flows uniformly (in the $-z$ direction) through the junction, i.e., that the junction is not self-field limited. We further assume that the currents into and out of the junction flow uniformly along the surface of the superconducting strips. This is a reasonable approximation in the junction region because the lower strip tends to act as a ground plane to the upper strip and vice versa.[28] Each opposing plane thus carries an equal and opposite screening current.

The currents flowing in the superconducting strips of the junction are[34,35]

$$I(x) = (\tfrac{1}{2} - x/w)i\,, \quad |x| \leq w/2$$

and (4.1)

$$I(y) = (\tfrac{1}{2} + y/w)i\,, \quad |y| \leq w/2$$

where i is the total junction current. The magnetic fields in the junction associated with these currents and their images are

$$H_x(y) = (4\pi i/cw)(\tfrac{1}{2} + y/w)\,,$$
$$H_y(x) = H_0 + (4\pi i/cw)(\tfrac{1}{2} - x/w)\,, \quad (4.2)$$

and

$$H_z = 0\,.$$

The phase difference across the junction, $\phi(x, y)$, is related to these fields by the equations[5,6] $\partial\phi/\partial x = (2ed/\hbar c)H_y$, $\partial\phi/\partial y = -(2ed/\hbar c)H_x$, where $d = 2(a+\lambda)$. Combining these equations with Eqs. (4.2), we obtain

$$\phi(x, y) = \alpha + \frac{2ed}{\hbar c}\left[H_0 x + \frac{2\pi i}{c}\left(\frac{x}{w} - \frac{x^2}{w^2}\right) - \frac{2\pi i}{c}\left(\frac{y}{w} + \frac{y^2}{w^2}\right)\right], \quad (4.3)$$

where α is a constant of integration. The current will be given by[5]

$$i = j_1 \operatorname{Im}\int_{-w/2}^{w/2} dx \int_{-w/2}^{w/2} dy\, e^{i\phi(x,y)}\,, \quad (4.4)$$

where j_1 is the maximum Josephson supercurrent per unit area. The critical current is found by maximizing Eq. (4.4) with respect to α. We can obtain a first approximation to the critical current by neglecting the squared terms in Eq. (4.3), upon which Eq. (4.4) may be integrated directly. The critical current is

$$i_c = j_1 w^2 \left|\frac{\sin[2\pi e d i_c/(\hbar c^2)]}{[ed/(\hbar c)]^2 (2\pi i_c/c)(2\pi i_c/c + wH_0)}\right|\,. \quad (4.5)$$

We assume that for $i > i_c$, there is a modulation of the supercurrent flowing at finite voltages of the form of Eq. (4.5), with $i_c = i$. We should expect to find oscillations whose period for $H = 0$ is $\Delta i \sim \hbar c^2/2ed \sim 3$ mA. This value is in sensible agreement with the experimentally observed values. It is not clear what determines the amplitude of the oscillation, or to what voltage they extend on the i-v characteristics. These effects are not observed in junctions with low critical currents, presumably because the supercurrent contribution at finite voltages is small, and the modulation amplitude too low to be detected. In the junctions in which the effects are observed, some degree of self-field limiting is always present. Under these circumstances, the finite-voltage supercurrent

arises chiefly from the middle regions of the junction, as pointed out in Sec. III C. The effect of the self-field in these regions is probably much less than in the outer regions, a fact which might explain the low amplitude.

The effect of a magnetic field will be to change the modulation from the form $[(\sin x)/x]^2$ into the form $[\sin(x)\sin(x+\delta)]/x^2$. The form and period of the oscillations will therefore be changed. This result is qualitatively correct, as may be seen from Fig. 6, but no quantitatively interpretable behavior has been observed.

It has proved possible to eliminate these oscillations from all junctions examined simply by using a symmetric current feed, which greatly reduces the self-field in the junction. For the symmetric case, Eqs. (4.1) become

$$I(x) = -(x/w)i, \quad |x| \le w/2$$

and (4.6)

$$I(y) = (y/w)i, \quad |y| \le w/2 .$$

The corresponding magnetic fields lead to a phase difference, which is just Eq. (4.3) with the linear terms in x and y deleted ($H_0 = 0$). The critical current is then of the form

$$I_c = j_1 w^2 \frac{[C(x)]^2 + [S(x)]^2}{x^2} , \qquad (4.7)$$

where $x = (2edi/\hbar c^2)^{1/2}$, and $C(x)$ and $S(x)$ are Fresnel integrals.[36] The function $F(x) \equiv \{[C(x)]^2 + [S(x)]^2\}/x^2$ is plotted in Fig. 8, together with $[(\sin x)/x]^2$. It will be seen that the first minimum of $F(x)$ occurs near the fourth minimum of $[(\sin x)/x]^2$. Since the oscillations for asymmetric inputs rarely extend to the fourth oscillation, it is reasonable to expect that no oscillations would be observed for symmetric inputs. However, a considerable distortion of the i-v characteristic near the origin might be expected. The discrepancies between theory and experiment noted in Sec. III B may arise from these self-field effects.

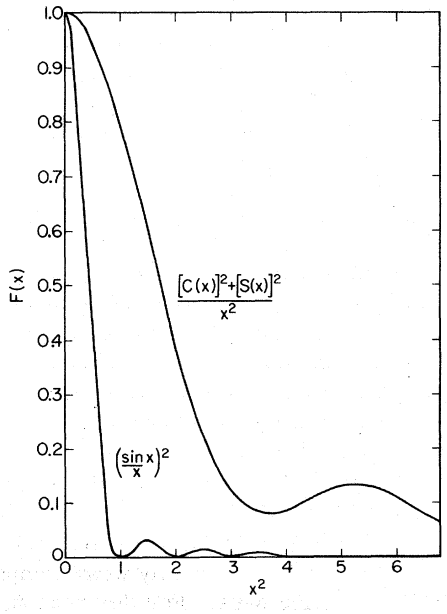

FIG. 8. Functions $F(x) \equiv [(\sin x)/x]^2$ and $F(x) \equiv \{[C(x)]^2 + [S(x)]^2\}/x^2$.

This self-field modulation of the i-v characteristic should be present in any type of junction in which there is a supercurrent contribution to the total current flowing at finite voltages. One should therefore be a little wary of interpreting every "bump and wiggle" on the i-v characteristic as a significant fundamental effect until self-field effects have been eliminated or allowed for. Particularly in high-resolution differential measurements, the self-fields may give rise to substantial distortion of the i-v characteristic, and obscure other more important effects.

V. EFFECT OF rf RADIATION

A. Form of Induced Steps

It is well known that the application of an oscillating electromagnetic field to a Josephson junction or weak link generates constant-voltage current steps on the i-v characteristic.[5,37] In a junction with an oxide barrier, the steps appear whenever the angular frequency of the applied radiation Ω, or a multiple of it, is equal to the angular frequency of the Josephson ac supercurrent $\omega = 2ev/\hbar$. The two frequencies then beat together to produce a zero frequency contribution to the supercurrent flowing at voltages[38] $v_n = n\hbar\Omega/2e$. In the case of a Dayem bridge,[39,40] "subharmonic" steps are also observed at voltages $v_{nm} = (n/m)\hbar\Omega/2e$.

Both harmonic and "subharmonic" steps have also been observed in *SNS* junctions. Typical i-v characteristics are shown in Figs. 9(a) and 9(b). The frequency range of applied radiation was a few kHz to 2 MHz. The radiation was applied in one of three ways: by passing an ac current through a small solenoid in which the junction was placed; by passing the ac current directly through the junction itself; or by passing the ac current along one of the superconducting strips forming one side of the junction. The first method was usually preferred because it eliminated the necessity of making direct connections to the junctions. In all three ways, the coupling was almost certainly magnetic. At the frequencies in question, the reactances of the junction inductance and capacitance were quite negligible compared with the resistance of about 10^{-6} Ω. The effective source impedance of the ac was many orders of magnitude greater than the junction resistance and we may safely assume that we have an ac current source rather than a voltage

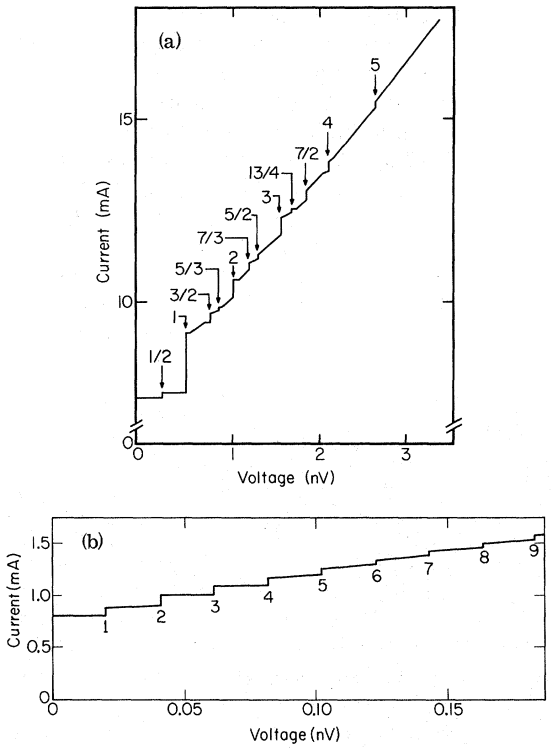

FIG. 9. Constant-voltage steps induced on *SNS* junctions. (a) $w/\lambda_J = 6.6$ and the applied frequency = 0.25 MHz. (b) $w/\lambda_J = 2.0$ and the applied frequency = 9.9 kHz. Asymmetric current inputs were used in both cases.

source. The i-v characteristics of the junctions were plotted as before, using a superconducting voltmeter in a null-reading mode. The loading of the junction by the voltmeter was negligible. The dc supplies were also current sources.

It was emphasized in II that the impedances of both ac and dc sources are crucial in determining the form of the induced step structure. If both sources are current sources, as they have been for all experiments on *SNS* junctions, then for the small junction limit Eq. (3.1) may be modified to include the effects of an rf field by adding to the left-hand side of a term $j_{rf}\sin\Omega t$, where j_{rf} is the amplitude of the rf current flowing through the junction. Equation (3.3) for the large junction limit is similarly modified by adding a term $(j_{rf}/i_c)\sin\Omega t$ to the left-hand side. These two equations have been solved numerically to obtain the i-v characteristics. It was shown in II that for a given value of current i the voltage in the presence of an rf field of frequency Ω was always a multiple or submultiple of $\hbar\Omega/2e$. Ideally, the whole i-v characteristic consists of a series of points at voltages $(n/m)\hbar\Omega/2e$. For small values of n and m, many points may have the same value of n/m and therefore form an induced step. The mathematical origins of this result are discussed in detail in II and will not be further described here.

The physical interpretation of this result is simple. We have seen in Sec. III that if ϕ is increasing in time in a uniform manner, as it is when an *SNS* junction is fed from a current source, the current-time relation will be nonsinusoidal. The junction will therefore generate harmonics, $\omega_m = m\omega$, when it is biased at a voltage $v = \hbar\omega/2e$. These harmonics may also synchronize with the applied radiation to produce steps. One therefore expects to see "subharmonic" steps, although it is clear that these steps arise from *harmonic* generation within the junction. The amplitude of the harmonics for large values of m is expected to be small so that the corresponding induced steps will be blurred out by thermal fluctuations and not observed. It should be emphasized that the observation of subharmonic steps does not imply a violation of the relation $i = i_c\sin\phi$ but rather indicates that ϕ is increasing with time in a nonlinear manner. In junctions with oxide barriers, the junction resistance is shunted by a parallel capacitance which usually has a much smaller impedance at the microwave frequencies used. The junction sees an ac *voltage* source and subharmonic steps are not observed. Sullivan *et al.*[41] have given a similar discussion on the origin of subharmonic steps in point contacts.

Two examples of rf-induced steps appear in Figs. 9(a) and 9(b). In Fig. 9(a), the applied frequency was about 0.25 MHz, and an abundance of harmonic and subharmonic steps is visible up to $n = 5$. In Fig. 9(b), the applied frequency was 9.9 kHz, corresponding to a step spacing of about 2.05×10^{-11} V. No subharmonic structure is visible but harmonic steps are present out to at least $n = 9$. The absence of subharmonic structure is probably due to the small amplitude of the harmonic currents produced by the junction, which has a low critical current. The characteristic tends to "jump" between the larger harmonic steps so that any low-amplitude subharmonic steps are obliterated.

It was found that if the dc current was fed symmetrically into the junction, the amplitude of the steps induced by an rf field in the solenoid was smaller than if the current was fed asymmetrically. This effect can be qualitatively explained by reference to the one-dimensional junction of Fig. 3. Assume that the rf field couples its magnetic field (in the y direction) to the magnetic fields generated by the currents in the lead strips in the vicinity of the junction. The coupling to the symmetrically biased junction is then relatively weak compared with the asymmetric case. For this reason, all data were taken with an asymmetric dc bias current.

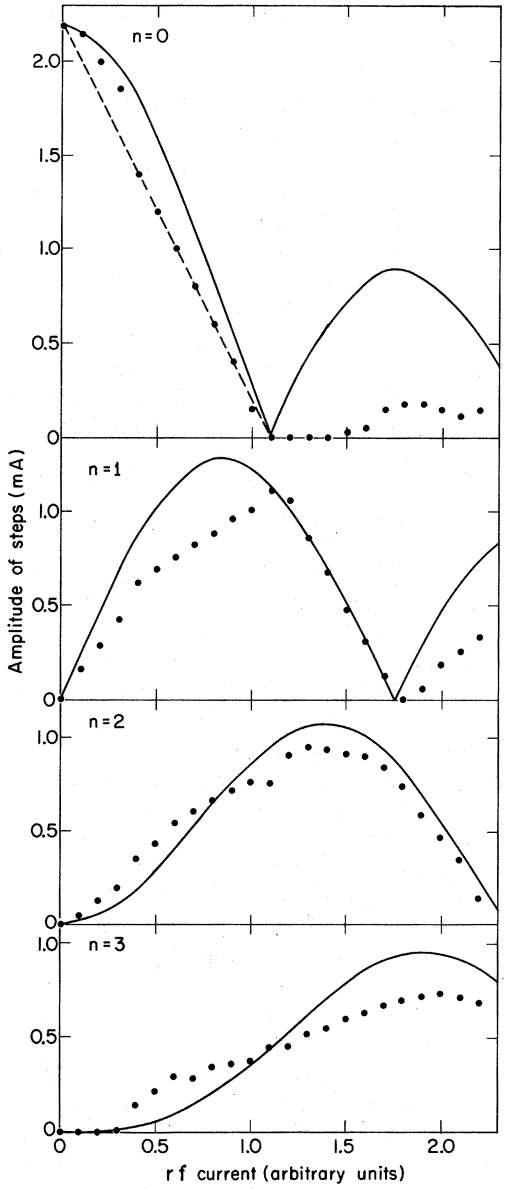

FIG. 10. Amplitude of induced steps, $n=0$, 1, 2, and 3, as a function of rf field. The frequency was 99.6 kHz, an asymmetric dc current feed was used, and the applied dc magnetic field was zero. The points represent experimental data and the curves the Bessel functions J_n. The theoretical curves were fitted at zero rf and the first minimum of $n=0$. The dashed line for $n=0$ corresponds to rectification.

B. Dependence of Step Amplitude on Magnitudes of Magnetic Field and rf Field

Figure 10 shows the dependence of the step amplitude upon the magnitude of the rf current in the solenoid for $n=0$, 1, 2, and 3. It was unfortunately not possible to obtain data at higher levels of rf because the superconducting voltmeter became inoperative in high rf fields. It can be seen, however, that both the $n=0$ and $n=1$ steps oscillate as a function of rf current.

We have no general analytic result for the dependence of step amplitude on the level of rf excitation for the case of current sources. However, for very small i_c, it can be shown (see II, p. 274) that the harmonic steps have amplitudes given approximately by

$$i_n = \frac{4 i_c e R}{\hbar \Omega} \left| J_n\left(\frac{2 j_{rf} e R}{\hbar \Omega}\right) \right| , \qquad (5.1)$$

where J_n is the Bessel function of order n, and R is the junction resistance. Equation (5.1) is analogous to the result obtained for constant voltage sources.[5] In Fig. 10, we have compared Eq. (5.1) with our experimental data, although there is little *a priori* justification for assuming the result will be valid for large i_c. We have written Eq. (5.1) in the form $j_0 |J_n(K_1 j_{rf})|$. The constant j_0 was obtained from the value of the $n=0$ step ($2i_c$) in the absence of rf excitation, and K_1 from the first zero of the $n=0$ step. The same values of j_1 and K_1 were used for the curves for $n=1$, 2, and 3.

The agreement around the second maximum of the $n=0$ step is poor, but elsewhere it is acceptable. Closer examination of the data points inside the first maximum of the $n=0$ step, i.e., $2i_c$, shows an almost linear dependence of amplitude upon j_{rf} (Fig. 10). It is interesting to ask whether the effect of the rf upon critical current is predominantly a rectifying process, as was found by Dayem and Wiegand[40] for Dayem bridges. Under these circumstances, the critical current $i_c(j_{rf})$ is given by the simple relation

$$i_c(j_{rf}) = i_c(0) - K_2 j_{rf} , \qquad (5.2)$$

where K_2 is a constant. We tested this result by measuring the rf current required to reduce i_c to zero for various values of i_c; i_c was varied by changing the temperature. The results are shown in Fig. 11, from which it appears that Eq. (5.2) is a reasonable approximation to the behavior of the junction. This result probably explains the low values of the data obtained under the second maximum of the zero-voltage step. However, if the effect of the rf were entirely a rectification process, there would always be a zero critical current for values of $K_2 j_{rf}$ greater than i_c.

We conclude that the effect of rf on the zero-voltage step is predominantly but not entirely a rectification process. The $n=1$, 2, and 3 induced steps appear to have a Bessel function dependence upon j_{rf}, although data at higher values of j_{rf} would be very desirable.

A magnetic field applied in the plane of the junction is expected to produce the "Fraunhofer modu-

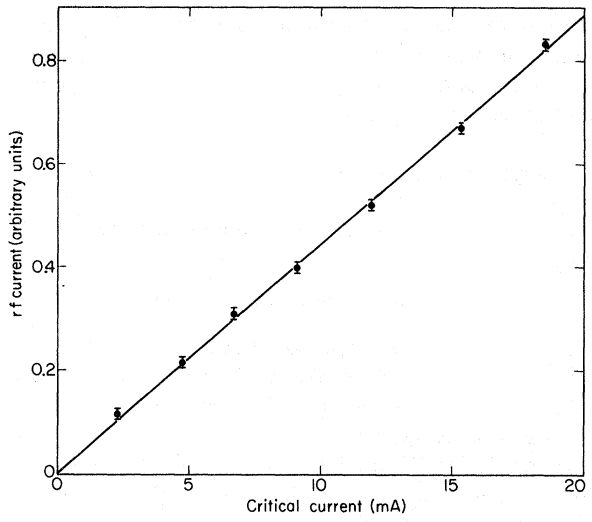

FIG. 11. Amplitude of rf field required to reduce the critical current to zero, as a function of critical current. Frequency of rf = 99.6 kHz, input asymmetric, zero applied dc magnetic field. The dots are experimental points and the straight line corresponds to a rectification process.

lation" of the critical current[4] and the induced steps.[5,42] Experimental data for the critical current in the absence of any rf excitation and the $n=0$, 1, 2, and 3 steps in the presence of a constant rf level are shown in Fig. 12. The skewing of the critical current vs magnetic field plot arises from the asymmetric dc current inputs.[27–29,34,35] The value of w/λ_J is 3.2 and the width of the central peak is greater than $2\phi_0$, indicating some degree of self-field limiting.[10] The amplitude modulation of the induced steps is highly asymmetric and generally confused. There are several regions over which the amplitudes are zero over an appreciable range of field. This effect is due to an "overlap" of the steps in current, so that the characteristic jumps from one step to the next at a somewhat arbitrary value of current. The steps are no longer independent under these conditions.

C. Dynamic Resistance of Induced Steps

It was found that the dynamic resistance of the induced steps was exceedingly low. The resistance was measured in the following way.[43,44] Two Pb-Cu-Pb junctions were connected in series with a superconducting thermal switch and a superconducting galvanometer[16] (see Fig. 13). The current resolution of the galvanometer was 0.3 μA,[45] and the inductance of the entire circuit L was $(1.0 \pm 0.1)\times 10^{-7}$ H. With the switch in the open position, steps were induced on each junction at a typical frequency of 0.5 MHz. Each junction was biased independently on the same order-induced step and the switch was closed. The circuit was then in a "differentially superconducting" state. Although there was a finite voltage (~1 nV) across the junctions, between X and Y in Fig. 13, an applied magnetic field B induced a circulating supercurrent provided that the amplitude of this supercurrent was not sufficient to drive either junction off its

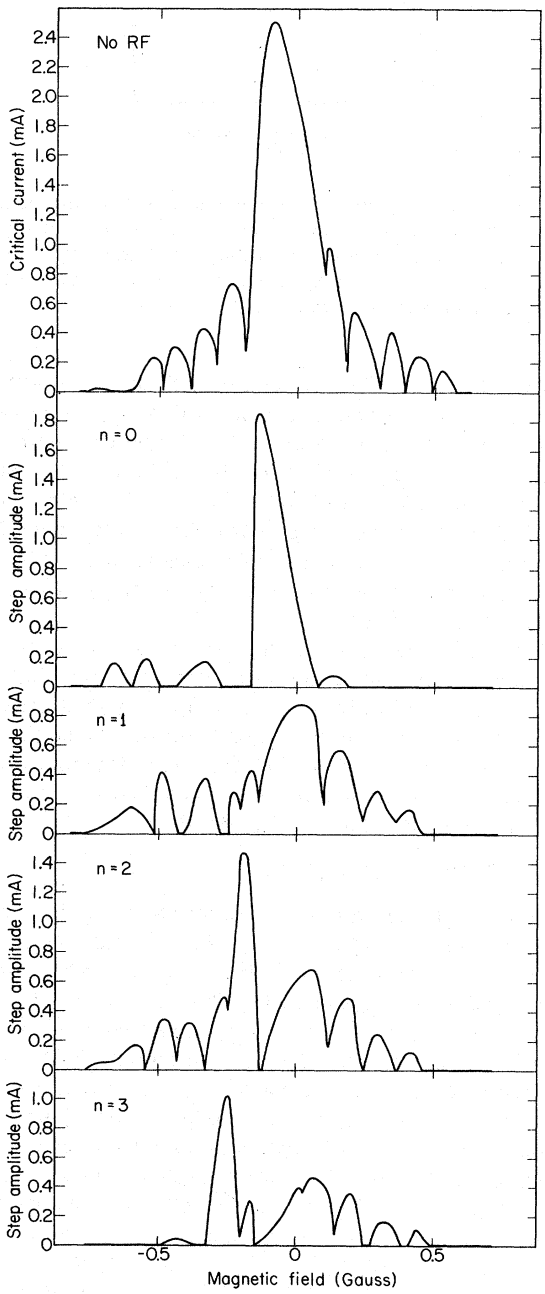

FIG. 12. The upper curve shows the variation of i_c with magnetic field (no rf excitation) with an asymmetric dc current input. The remaining four curves show the variation of the $n=0, 1, 2$, and 3 induced steps with magnetic field at a constant rf level (99.6 MHz). $w/\lambda_J = 3.2$.

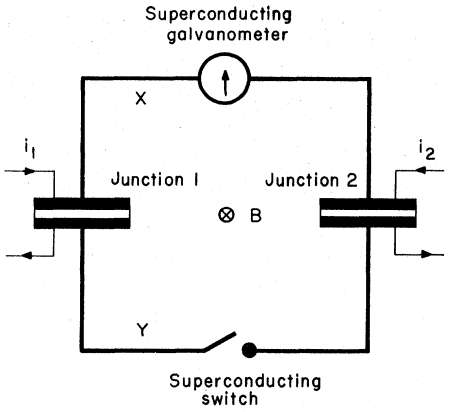

FIG. 13. Circuit used for measuring dynamic resistance of induced steps and comparing induced electrochemical potential on junctions of different materials. With the superconducting switch closed, the circuit is everywhere superconducting except for the junctions.

induced step. The rate of decay of this circulating supercurrent gives a measure of the dynamic resistance of the two steps. In a typical experiment, the circulating current was 0.5 mA, and the decay less than 0.3 μA in 1.8×10^3 sec. The time constant τ was therefore greater than 3×10^6 sec, the total circuit resistance (L/τ) less than 3.3×10^{-14} Ω, and the differential resistance per junction less than 1.7×10^{-14} Ω.

Detailed calculations have been carried out on the dynamic resistance of induced steps by Stephen[46] and in II, and in this paper we merely quote the results. At the center of an integer-order step, the dynamic resistance of the step R_s in terms of the dynamic resistance of the i-v characteristic in the absence of radiation R_D is given by

$$R_s/R_D=[I_0(j_s/i_N)]^{-2}\ . \tag{5.3}$$

Here, I_0 is the modified Bessel function, j_s is one-half the step height, and $i_N=2\pi kT/\phi_0$ is a characteristic noise current.[47] If $j_s\ll i_N$, I_0 can be approximated as an exponential. The noise current i_N may contain contributions from external noise sources so that the effective noise temperature is above the junction temperature. However, because of their exceedingly low impedance, *SNS* junctions do not couple well to external radiation, and it is probably reasonable to assume that the noise temperature is not too far from the bath temperature. At 4 K, i_N is rather less than 10^{-7} A. If we assume a step height $(2j_s)$ of 1 mA, we find R_s/R_D $\sim\exp(-10^4)$. Since $R_D\sim10^{-6}$ Ω, the value of R_s is of order 10^{-4000} Ω, very far below the observational limit. In a more detailed calculation, Stephen[46] has shown that the dynamic resistance of the step should increase towards its extremities. He finds that, for a 1-mA step at 500 kHz, the voltage should be greater than the midpoint value by 10^{-17} V at a point which is at about 97% of the half-step height. It is unfortunately not practicable to obtain experimental data at points so close to the top of the step.

It appears that, for most practical purposes, the steps may be regarded as having zero dynamic resistance, provided the step height is reasonably large.

D. Frequency Range of Induced Steps

It was found that steps could not be induced for frequencies above 1–2 MHz or below about 5 kHz. It is of interest to consider the reasons for these two limiting frequencies.

By analogy with the behavior in a bulk superconductor, one would expect the applied rf fields to penetrate into the junction for a distance given by the smaller of $2\lambda_J$ and the classical skin depth δ. As the frequency is increased, δ will decrease and the rf currents will be increasingly screened out of the junction and unable to couple to the Josephson supercurrents. If the barrier is of pure Cu for which the resistivity is typically 10^{-7} Ω cm, δ is equal to $\frac{1}{2}w$ at a frequency of about 0.5 MHz. One might expect a significant reduction in magnitude of the induced steps at frequencies somewhat higher than this figure, as is observed.

The lower-frequency limit, below which steps will not be observed, is set by thermal noise generated in the junction. This noise will give the Josephson frequency a finite linewidth $\Delta\nu$. The synchronization between the applied radiation of frequency $\Omega/2\pi$ and the Josephson ac supercurrent becomes increasingly disrupted by noise as $\Omega/2\pi$ is lowered towards $\Delta\nu$, and the step will be very blurred out when $\Omega/2\pi$ and $\Delta\nu$ are comparable. Dahm *et al.*[48] showed that for tunnel junctions at voltages much less than kT/e, the linewidth of the Josephson radiation may be written as

$$\Delta\nu=4\pi kTR_D^2/\phi_0^2R_S\ . \tag{5.4}$$

R_D is the dynamic resistance of the junction $(\partial v/\partial i)$, and R_S is the static resistance (v/i). Kanter and Vernon[49] found that this result was approximately correct for point-contact junctions. We assume that Eq. (5.4) also holds for an *SNS* junction, although this assumption is by no means justified *a priori*. For a junction with a critical current of about 1 mA, and with an applied frequency of 5 kHz, corresponding to a voltage of about 10^{-11} V, R_S is about 10^{-8} Ω. If we take $T\sim4$ K, and $R_D\sim5\times10^{-7}$ Ω, we find from Eq. (5.4) that $\Delta\nu$ ~5 kHz. This bandwidth does correspond to the lowest frequency at which steps can be seen, although the good agreement is undoubtedly somewhat fortuitous.

E. Effects of Junction Materials and Experimental Conditions on the Josephson Voltage-Frequency Relation

In view of the use of the ac Josephson effect in the determination of fundamental constants,[50] and in the comparison of standards of emf,[51] it is important to establish experimentally that the value of the electrochemical potential at which the steps appear, for a given frequency, is independent of the junction material and the experimental conditions. There are excellent theoretical grounds for believing this result to be true.[50] A simple comparison experiment was performed[43,44] to verify to 1 part in 10^8 the accuracy of the Josephson relation $\hbar\omega = 2\Delta\mu$, where $\Delta\mu$ is the electrochemical potential difference across the junction.

The experimental configuration was again that of Fig. 13, but the junctions were of different materials, for example, lead and tin. The junctions were biased as in Sec. V C, and the superconducting switch closed, but no circulating supercurrent was induced around the ring. Instead, the galvanometer was observed for a period of time to see whether or not a supercurrent slowly developed. If we assume that the induced steps occur at different electrochemical potentials, $\Delta\mu_1$ and $\Delta\mu_2$, then a supercurrent j would be induced in the circuit at a rate

$$L\frac{dj}{dt} = \frac{\Delta\mu_1 - \Delta\mu_2}{e} \quad . \tag{5.5}$$

After 30 min, j was observed to be zero to within the galvanometer resolution, 0.3 μA. Taking $L = 10^{-7}$ H, we find, from Eq. (5.5), that $|\Delta\mu_1 - \Delta\mu_2|/e < 1.7\times10^{-17}$ V. At 1 Mhz, for which $\Delta\mu_1/e \sim 2$ nV, this value corresponds to $|\Delta\mu_1 - \Delta\mu_2|/\Delta\mu_1 < 10^{-8}$.

In a variation of this experiment, a very small resistance, about 10^{-10} Ω, was inserted in series with the galvanometer. The comparison then becomes a voltage measurement, although the time constant is very long, of order 10^3 sec. The junctions were biased as before and the superconducting switch closed. After 30 min, or about two time constants, no current could be detected by the galvanometer. This measurement corresponds to a resolution of 3×10^{-17} V. At 1 MHz, the result implies that the electrochemical potentials of the two steps were identical to $1\frac{1}{2}$ parts in 10^8.

The same null results were obtained when the pairs of superconductors were lead and indium, or tin and indium, and also when silver was substituted for Cu in one of the junctions. In addition, the variation of the following parameters, although generally affecting the shape of the current-voltage characteristic and the amplitude of the steps, did not give rise to any observable difference in electrochemical potential across the junctions: (i) temperature, from 1.2 to 2.2 K (variation of temperature produces changes in energy gap, coherence length, etc.); (ii) barrier thickness from 0.5 to 1.4 μ; (iii) level of rf amplitude, over a factor of 5; (iv) rf frequency, from 100 kHz to 1 MHz (to 1 part in 10^7 at 100 kHz); (v) the order of induced steps on which both steps were biased, up to $n = 4$; (vi) the position on the induced step, up to 75% of the half-step height; (vii) the ambient magnetic field, up to ± 1 G; (viii) the direction of the bias current through the junctions.

It has therefore been shown that the electrochemical potential at which steps appear at a given frequency is independent of the junction material and the experimental conditions to 1 part in 10^8. This result is a useful one, because if there are no *differences* in possible corrections for different materials and for different conditions to 1 part in 10^8, there is a good chance that there are no significant corrections at all to 1 part in 10^6, at which level of accuracy the absolute value is required.

F. Use of Induced Steps as Voltage Standards

We have frequently had cause to calibrate resistances of 10^{-8} Ω or less at liquid-helium temperatures. This calibration may be readily achieved by using the induced steps on *SNS* junctions as accurately known voltage standards in the helium bath.

VI. SUMMARY

We have shown that most of the details of the behavior of *SNS* junctions are well understood. The critical current is adequately represented by a relation having the form of Eq. (1.2), and its modulation by a magnetic field is as predicted. The i-v characteristics of small junctions are in good agreement with theory. The finite-voltage behavior of large junctions, in which there is a substantial dc supercurrent at large voltages, is understood qualitatively. However, the value of w/λ_J at which flux flow begins is found experimentally to be about 2 rather than the theoretical value of 4. The magnitude of the finite-voltage dc supercurrent is appreciably greater experimentally than the theoretical prediction. Both of these discrepancies probably arise from the comparison of a two-dimensional junction with a one-dimensional model. It would be of interest to study one-dimensional junctions.

A form of self-modulation of the i-v characteristic has been observed and accounted for qualitatively. Other junctions in which there is a finite-voltage dc supercurrent should exhibit the same phenomenon.

The application of rf fields to the junction induces constant-voltage current steps on the i-v characteristic, over a frequency range of 5 kHz to 2 MHz. These steps have an exceedingly low dynamic resistance, provided that the amplitude is reasonably

large. The amplitude of the steps is modulated by varying the amplitude of the rf excitation or by varying the static magnetic field. The electrochemical potential at which these steps appear is independent of the junction material and experimental conditions to an accuracy of 1 part in 10^8.

ACKNOWLEDGMENTS

I gratefully acknowledge several helpful discussions with Professor A. B. Pippard, F. R. S., Dr. J. R. Waldram, and Paul K. Hansma.

*Work performed under the auspices of the U.S. AEC.

†Alfred P. Sloan Foundation Fellow.

[1]P. G. de Gennes and E. Guyon, Phys. Letters 3, 168 (1963).

[2]P. G. de Gennes, Rev. Mod. Phys. 36, 225 (1964).

[3]P. G. de Gennes, *Superconductivity of Metals and Alloys* (Benjamin, New York, 1966).

[4]P. W. Anderson and J. M. Rowell, Phys. Rev. Letters 10, 230 (1963).

[5]B. D. Josephson, Advan. Phys. 14, 419 (1965).

[6]P. W. Anderson, in *Lectures on the Many-Body Problem*, edited by E. R. Caianiello (Academic, New York, 1964), Vol. 2, p. 115.

[7]B. D. Josephson, Rev. Mod. Phys. 36, 216 (1964).

[8]B. D. Josephson, Phys. Letters 1, 251 (1962).

[9]B. D. Josephson, Fellowship thesis (Trinity College, Cambridge, England, 1962) (unpublished).

[10]J. Clarke, Proc. Roy. Soc. (London) A308, 447 (1969); a brief account also appeared in J. Phys. (Paris) Colloq. Suppl. C2, 2 (1968).

[11]R. A. Ferrell and R. E. Prange, Phys. Rev. Letters 10, 479 (1963).

[12]λ is increased above its bulk value (Ref. 3) because the pair density in the superconductor is depressed by the proximity of the normal metal. The over-all correction to $a+\lambda$ below $\frac{1}{2}T_{cS}$ is small, not greater than 5%.

[13]C. S. Owen and D. J. Scalapino, Phys. Rev. 164, 538 (1967).

[14]S. I. Bondarenko, I. M. Dmitrenko, and E. I. Balanov, Fiz. Tverd. Tela 12, 1417 (1970) [Sov. Phys. Solid State 12, 1113 (1970)].

[15]J. R. Waldram, A. B. Pippard, F.R.S., and J. Clarke, Phil. Trans. Roy. Soc. London 268, 265 (1970); a brief account of this work was given at the Conference on the Science of Superconductivity, Stanford University, California (unpublished).

[16]J. Clarke, Phil. Mag. 13, 115 (1966).

[17]G. I. Rochlin, Rev. Sci. Instr. 41, 73 (1970).

[18]External noise radiated into the cryostat or carried in by cryostat leads may give an effective noise temperature which is much greater than the bath temperature.

[19]A more detailed account of this model was given by the author in *Proceedings of the Twelfth International Conference on Low Temperature Physics, Kyoto*, edited by E. Kauda (Academic Press of Japan, Kyoto, Japan, 1970), p. 443.

[20]J. Bardeen, L. N. Cooper, and J. R. Schrieffer, Phys. Rev. 108, 1175 (1957).

[21]A. F. Andreev, Zh. Eksperim. i Teor. Fiz. 46, 1823 (1964) [Sov. Phys. JETP 19, 1228 (1964)].

[22]W. L. McMillan, Phys. Rev. 175, 559 (1968).

[23]A. B. Pippard, F.R.S., J. G. Shepherd, and D. A. Tindall, Proc. Roy. Soc. (London) A324, 17 (1971).

[24]Preliminary measurements of this effect were reported by the author in his Ph.D. thesis (Christ's College, Cambridge, 1967) (unpublished). A very detailed account is given in Ref. 23.

[25]D. E. McCumber, J. Appl. Phys. 39, 3113 (1968).

[26]L. G. Aslamazov, A. I. Larkin, and Yu. N. Ovchinnikov, Zh. Eksperim. i Teor. Fiz. 55, 323 (1968) [Sov. Phys. JETP 28, 171 (1969)].

[27]A. M. Goldman and P. J. Kreisman, Phys. Rev. 164, 544 (1967).

[28]J. Matisoo, J. Appl. Phys. 40, 1813 (1969).

[29]K. Schwidtal, Phys. Rev. B 2, 2526 (1970).

[30]We cannot directly estimate values of $w/\lambda_J > 4$ from the observed critical current because this value is less than the true value. The true values of λ_J were estimated by experiments on junctions of different areas (see I, Fig. 8).

[31]D. E. McCumber, J. Appl. Phys. 39, 2503 (1968).

[32]W. C. Stewart, Appl. Phys. Letters 12, 277 (1968).

[33]J. Clarke and T. A. Fulton, J. Appl. Phys. 40, 4470 (1969).

[34]T. Yamashita and Y. Onodera, J. Appl. Phys. 38, 3523 (1967).

[35]K. Schwidtal and R. D. Finnegan, J. Appl. Phys. 40, 2123 (1969).

[36]See, for example, *Handbook of Mathematical Functions*, edited by M. Abramowitz and I. A. Stegun (Dover, New York, 1965).

[37]S. Shapiro, Phys. Rev. Letters 11, 80 (1963).

[38]The Josephson voltage-frequency relation is properly written $\hbar\omega = 2\Delta\mu$, where $\Delta\mu$ is the electrochemical potential difference across the junction. We shall assume in this discussion that the only contribution to $\Delta\mu$ is from the electrostatic potential, $v = \Delta\mu/e$, and that contributions from thermal gradients, stress gradients, etc., are negligible. The potentiometer used to measure the "voltage" of the induced steps, of course, measures $\Delta\mu/e$ rather than v, so that any other terms are properly included in the measurement.

[39]P. W. Anderson and A. H. Dayem, Phys. Rev. Letters 13, 195 (1964).

[40]A. H. Dayem and J. J. Wiegand, Phys. Rev. 155, 419 (1967).

[41]D. B. Sullivan, R. L. Peterson, V. E. Kose, and J. E. Zimmerman, J. Appl. Phys. 41, 4865 (1970).

[42]T. Yamashita and Y. Onodera, J. Appl. Phys. (Japan) 6, 746 (1967). These authors point out that one obtains a qualitatively different behavior when the magnetic field is parallel to the direction of microwave propagation than when it is at right angles to it. Their argument applies when $w > \lambda$, where λ is the microwave wavelength. In the present experiments, $w \ll \lambda$, and there is no difference in the two cases. This result has been verified experimentally by applying the static field both parallel to and at right angles to the rf magnetic field, both fields being in the plane of the junction.

[43]J. Clarke, Phys. Rev. Letters 21, 1566 (1968).

[44]J. Clarke, in *Proceedings of the Eleventh International Conference on Low Temperature Physics*, edited by J. F. Allen, D. M. Finlayson, and D. M. McCall (St. Andrews U.P., St. Andrews, Scotland, 1969), p. 95.

[45]rf pickup reduced the galvanometer sensitivity somewhat.
[46]M. J. Stephen, Phys. Rev. 186, 393 (1969).
[47]A factor of π was omitted from the expression for i_N in II.
[48]A. J. Dahm, A. Denenstein, D. N. Langenberg, W. H. Parker, D. Rogovin, and D. J. Scalapino, Phys. Rev. Letters 22, 1416 (1969).
[49]H. Kanter and F. L. Vernon, Jr., Phys. Rev. Letters 25, 588 (1970).
[50]W. H. Parker, D. N. Langenberg, A. Denenstein, and B. N. Taylor, Phys. Rev. 177, 639 (1969). For a review and further references, see J. Clarke, Am. J. Phys. 38, 1071 (1970).
[51]B. N. Taylor, W. H. Parker, D. N. Langenberg, and A. Denenstein, Metrologia 3, 89 (1967).

PHYSICAL REVIEW B VOLUME 4, NUMBER 9 1 NOVEMBER 1971

Study of Supercooling and Thermal Conductivity in Superconducting Molybdenum†

A. Waleh and N. H. Zebouni
Department of Physics and Astronomy, Louisiana State University, Baton Rouge, Louisiana 70803
(Received 10 June 1971)

The critical magnetic field and the associated supercooling are measured and analyzed in superconducting molybdenum. The coexistence of a superconducting surface sheath with a supercooled normal bulk is confirmed. Thermal-conductivity measurements are analyzed and the possible influence of s-d scattering close to T_c is discussed.

I. INTRODUCTION

Superconductivity in the transition metals has been the subject of many experimental and theoretical investigations in recent years. Many of the experiments and observations on this group of elements, in particular, studies of the absence or considerable reduction of the isotope effect,[1] the pressure dependence of the transition temperature T_c,[2] the relation of T_c to the total density of states at the Fermi surface,[3] the effect of magnetic impurities,[4] and the empirical rules relating T_c to the position in the Periodic Table,[5] have led some of the investigators[6] to suggest mechanisms different from the electron-phonon interaction, as originally proposed by Bardeen *et al.*[7] (BCS), to be partially responsible for superconductivity in the transition metals. On the theoretical side, however, in the spirit of a two-band model for the electronic structure of the transition metals[8] and assuming the Fermi surface separable into s- and d-like regions, it has been shown by Garland[9] that experimentally observed superconducting properties of the transition metals could be explained by a single-gap theory appropriate to dirty[10] materials. Based on his model and the single-gap theory, Garland[11] has carried out calculations of the isotope effect coefficients in the limit of sufficient dirtiness[12] and has shown that the experimental evidence supports the BCS theory and the idea of phonon-induced superconductivity. Although the superconducting state parameters have been calculated[13] using the electron-phonon interaction and were found to be in agreement with the experimental results, the present knowledge of the electronic-band structure of the transition metals is insufficient to resolve the controversy and completely justify the theoretical models.

Much of the success of the experiments on transition metals is due to the recent purification techniques. In fact, elements such as molybdenum can be sufficiently pure to show the characteristics of a "clean" superconductor.[9,10] Thus, it seems of interest to carry out further experimental investigations of the superconducting transition and of the transport properties of molybdenum, particularly below 1 °K where molybdenum becomes superconducting. In this temperature region, for a pure metal, one can safely assume that the heat conductivity is predominantly electronic. Also, since molybdenum has a very high Debye temperature relative to its superconducting transition temperature and because of a large electronic mean free path due to its high purity, one may expect the scattering of the electrons by thermally excited lattice vibrations to be negligible as compared to their elastic scattering by static imperfections such as impurities, lattice defects, or, at even lower temperatures, by the boundaries. In turn, in a very pure transition metal one can hope to see some influence of another scattering process: the electron-electron scattering or s-d scattering. Under these conditions, the study of the thermal conductivity of molybdenum in the normal and superconducting states will prove very useful for comparison with the theory of Bardeen, Rickayzen, and Te-